

# Synchronization and Anti-synchronization of Coupled Hindmarsh–Rose Neuron Models

Christos K. Volos<sup>†</sup>, Dimitrios Prousalis<sup>†</sup>, Ioannis M. Kyprianidis<sup>†</sup>, Ioannis Stouboulos<sup>†</sup>,  
Sundarapandian Vaidyanathan<sup>1</sup>, and Viet-Thanh Pham<sup>‡</sup>

**Abstract:** In this paper, a coupling scheme based on Nonlinear Open Loop Controllers, between two identical coupled Hindmarsh–Rose neuron models is investigated analytically and numerically. In more details the cases of bidirectional and unidirectional coupling are chosen, which are designed for achieving two of the more interesting types of synchronization the complete synchronization and anti-synchronization. The stability of the proposed method is ensured by using the Lyapunov function stability theory. Simulation results verified that the proposed coupling scheme drives the system either to complete synchronization or anti-synchronization depending on the choice of the signs of the error function's parameters. Furthermore, the Hindmarsh–Rose neuron model is emulated by an electronic circuit and its dynamical behavior is studied by using the electronic simulation package Cadence OrCAD in order to confirm the feasibility of the theoretical model.

**Keywords:** Chaos, Hindmarsh–Rose neuron model, synchronization, antisynchronization, nonlinear open loop controller, bidirectional coupling, unidirectional coupling.

## 1. INTRODUCTION

Today is known that neurons are the core component of the nervous system. Organized internally similar to other cells, they are specialized for intercellular communication by way of their membrane potential. Biological experiments and numerical analysis of models for the oscillations of isolated neurons, have led the researchers to construct low dimensional analog electronic neurons which properties are designed to emulate the membrane voltage characteristics of the individual neurons. So, in the case of modeling a biological neuron, physical analogues are used in place of abstractions such as “weight” and “transfer function”. The input to a neuron is often described by an ion current through the cell membrane that occurs when neurotransmitters cause an activation of ion channels in the cell. We describe this by a physical time-dependent current  $I(t)$ . The cell itself is bound by an insulating cell membrane with a concentration of charged ions on either side that determines a capacitance  $C_m$ . Finally, a neuron responds to such a signal with a change in voltage, or an electrical potential energy difference between the cell and its surroundings, which is observed sometimes as a voltage spike called an action potential. This quantity, then, is the quantity of interest and is given by  $V_m$ .

Until now, many models of biological neurons have been reported in literature, such as Hodgkin-Huxley and FitzHugh-Nagumo [1-5]. However, the Hindmarsh-Rose is the most studied neuron model because it exhibits all the computational properties of biological spiking neurons.

The Hindmarsh-Rose (HR) model is based on the global behavior of the neuron and its underlying operation is removed from the actual biological process. For this reason, it is one of the most interesting neuron models which is used for studying the neuronal activity and more specifically the spiking-bursting

<sup>†</sup> Physics Department, Aristotle University of Thessaloniki, Thessaloniki, Greece.

<sup>1</sup> Research and Development Centre, Vel Tech University, Avadi, Chennai, India.

<sup>‡</sup> School of Electronics and Telecommunications, Hanoi University of Science and Technology, Vietnam.

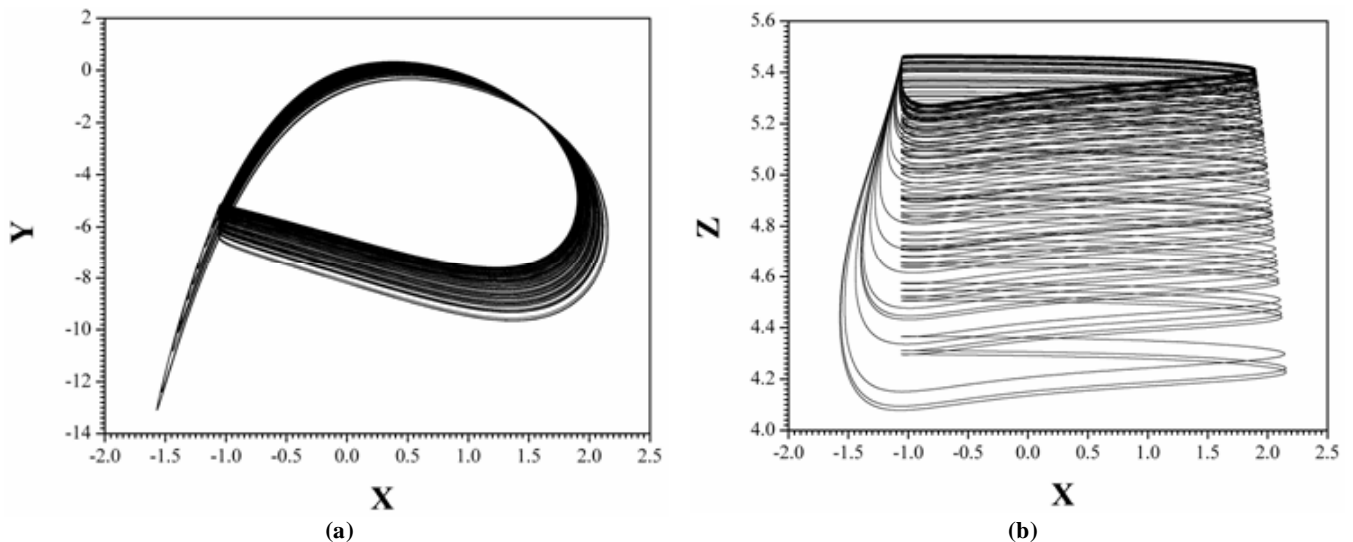
behavior of the membrane potential observed in experiments made with a single neuron. This phenomenological neuron model, which has been proposed by Hindmarsh and Rose [6], may be seen either as a generalization of the Fitzhugh equations or as a simplification of the physiologically realistic model proposed by Hodgkin and Huxley. It has been proven to be a single-compartment model providing a good compromise between two seemingly mutually exclusive requirements: The model for a single neuron must be both computationally simple, and capable of mimicking almost all the behaviors exhibited by real biological neurons, in particular the rich firing patterns [7].

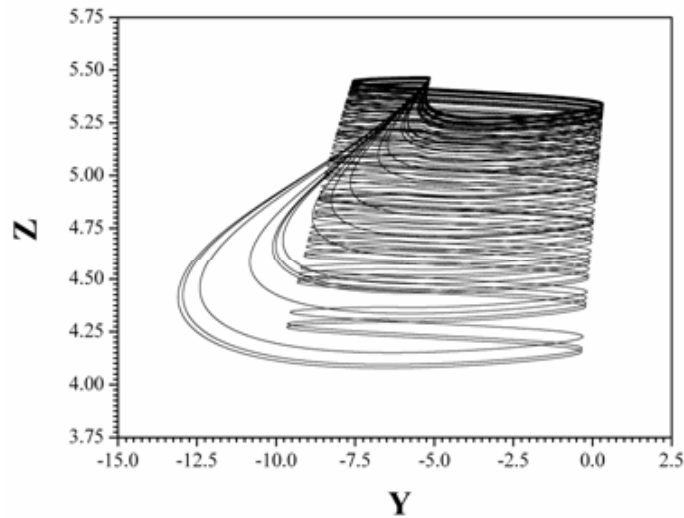
So, the three-variable HR model of action potential was proposed as a mathematical representation of the firing behavior of neurons, and it was originally introduced to give a bursting type with long InterSpike Intervals (ISIs) of real neurons. It can be used to simulate spiking/bursting and chaos phenomena in real neurons. The equations of the HR model are given as follows:

$$\begin{cases} \frac{dX}{d\tau} = Y - X^3 + aX^2 - Z + I \\ \frac{dY}{d\tau} = c - dX^2 - Y \\ \frac{dZ}{d\tau} = r(s(X + \chi) - Z) \end{cases} \quad (1)$$

where,  $X$  represents the membrane action potential,  $Y$  is a recovery variable and  $Z$  is a slow adaptation current;  $I$  mimics the membrane input current for the biological neurons;  $a, b$  allows one to switch between bursting and spiking behaviors and to control the spiking frequency;  $r$  controls the speed of variation of the slow variable  $Z$  in Eq.(1), (i.e., the efficiency of the slow channels in exchanging ions) and in the presence of spiking behaviors, it governs the spiking frequency, whereas in the case of bursting, it affects the number of spikes per burst;  $s$  governs adaptation: a unitary value of  $s$  determines spiking behavior without accommodation and sub-threshold adaptation, whereas values around  $s = 4$  give strong accommodation and sub-threshold overshoot, or even oscillations;  $\div$  sets the resting potential of the system. In Figure 1 the chaotic attractors of the Hindmarsh-Rose neuron system (1), for  $a = 3.1$ ,  $c = 1.2$ ,  $d = 5.8$ ,  $I = 6$ ,  $r = 0.01$ ,  $\chi = 1.9$  and  $s = 4.9$ , is shown. The system's chaotic behavior is verified by the calculation of system's Lyapunov exponents, which are  $\lambda_1 = 0.03705$ ,  $\lambda_2 = 0$  and  $\lambda_3 = -13.9890$ . As is known, the existence of a positive Lyapunov exponent is an indication of a chaos.

In this work, the cases of two bidirectionally and unidirectionally coupled identical Hindmarsh-Rose neuron models, by using a recently new proposed method (Nonlinear Open Loop Controllers) are studied.





(c)

**Figure 1: The chaotic attractors of Hindmarsh-Rose neuron model, for  $a = 3.1$ ,  $c = 1.2$ ,  $d = 5.8$ ,  $I = 6$ ,  $r = 0.01$ ,  $\chi = 1.9$  and  $s = 4.9$ , in (a)  $X - Y$  plane, (b)  $X - Z$  plane and (c)  $Y - Z$  plane.**

The simulation results from coupling system's numerical integration verify the appearance of the complete synchronization and antisynchronization phenomenon.

The paper is organized as follows. In Section 2 the cases of synchronization and antisynchronization between bidirectionally and unidirectionally coupled HR neuron models by using the nonlinear open loop controllers, are presented. Section 3 presents the simulation results which confirm the feasibility of the proposed coupling schemes while Section 4 shows the circuitual implementation of HR model. Finally, the conclusive remarks are drawn in the last Section.

## 2. THE COUPLING SCHEME

In the last three decades the phenomenon of synchronization between coupled chaotic systems has attracted the interest of the scientific community because it is a rich and multi-disciplinary phenomenon with broad range applications, such as in a variety of complex physical, chemical, and biological systems [8-14], as well as in secure communications [15], cryptography [16,17] and broadband communication systems [18]. In more detail, synchronization of chaos is a process, where two or more chaotic systems adjust a given property of their dynamics motion to a common behavior, such as identical trajectories or phase locking, due to coupling or forcing. Because of the exponential divergence of the nearby trajectories of a chaotic system, having two chaotic systems being synchronized, might be a surprise. However, today the synchronization of coupled chaotic oscillators is a phenomenon well established experimentally and reasonably well understood theoretically.

The history of chaotic synchronization's theory began with the study of the interaction between coupled chaotic systems in the 1980's and early 1990's by Fujisaka and Yamada [19], Pikovsky [20], Pecora and Carroll [21]. Since then, a wide range of research activity based on synchronization of nonlinear systems has risen and a variety of synchronization's types depending on the nature of the interacting systems and of the coupling schemes has been presented.

In particular, the phenomenon of complete synchronization is the most studied type of synchronization. In this case, two coupled chaotic systems are led to a perfect coincidence of their chaotic trajectories i.e.,

$$x(t) = y(t) \text{ as } t \rightarrow \infty \quad (2)$$

Another interesting phenomenon is the antisynchronization, in which two coupled systems  $x$  and  $y$ , can be synchronized in amplitude, but with opposite sign, for initial conditions chosen from large regions in the phase space, that is

$$x(t) = -y(t) \text{ as } t \rightarrow \infty \quad (3)$$

The coupling scheme between two identical Hindmarsh-Rose neuron models can be either unidirectional, in which the dynamics only of the first coupled neuron model affects the second one, or bidirectional, in which the dynamics of both coupled neuron models affects each other.

As it is mentioned, in this work, the following coupling scheme, described by the following system of differential equations:

$$\begin{cases} \dot{x} = f(x) + U_x \\ \dot{y} = f(y) + U_y \end{cases} \quad (4)$$

has been chosen.

In this system,  $(f(x), f(y)) \in R^n$  are the flows of the master and slave system respectively, while  $U_x$  and  $U_y$  are the Nonlinear Open Loop Controllers [22]. The error function is defined by  $e = \gamma y - \delta x$ , with  $e = [e_1, e_2, e_3, e_4]^T$ ,  $x = [x_1, x_2, x_3, x_4]^T$  and  $y = [y_1, y_2, y_3, y_4]^T$ .

If one applies the Lyapunov Function Stability (LFS) technique, a stable synchronization state will be realized when the error function of the coupled system follows the limit

$$\lim_{t \rightarrow \infty} \|e(t)\| \rightarrow 0 \quad (5)$$

so that  $\gamma x = \delta y$ .

As it is mentioned, the design process of the coupling scheme, is based on the Lyapunov function

$$V(e) = \frac{1}{2} e^T e \quad (6)$$

where  $T$  denotes transpose of a matrix and  $V(e)$  is a positive definite function. For known system's parameters and with the appropriate choice of the controllers  $U_x$  and  $U_y$ , the coupled system has  $\dot{V}(e) < 0$ . This ensures the asymptotic global stability of synchronization and thereby realizes any desired synchronization state.

By using the appropriate NOLCs functions  $U_x$ ,  $U_y$  and error function's parameters  $\gamma$ ,  $\delta$ , a unidirectional or bidirectional (mutual) coupling scheme can be implemented. In more details, for  $(U_x = 0, \delta = 1)$  or  $(U_y = 0, \gamma = 1)$ , a unidirectional coupling scheme is realized, while for  $U_{x,y} \neq 0$  and  $\gamma, \delta \neq 0$ , a bidirectional coupling scheme is realized, respectively. The signs of  $\gamma, \delta$  play a crucial role to the type of synchronization (complete synchronization or antisynchronization), which is observed in this work. On the other hand, the ratio of  $\gamma$  and  $\delta$  decides the amplification or attenuation of one oscillator relative to another one.

Next, the coupling schemes (bidirectional and unidirectional), by using the NOLCs functions are presented in details.

## 2.1. BIDIRECTIONAL COUPLING

In the first case, the bidirectional coupling scheme of two coupled HR systems of Eqs. (1), which is described by the following systems (7), (8), is studied.

Coupled System-1:

$$\begin{cases} \frac{dx_1}{dt} = x_2 - x_1^3 + ax_1^2 - x_3 + I + U_{x1} \\ \frac{dx_2}{dt} = c - dx_1^2 - x_2 + U_{x2} \\ \frac{dx_3}{dt} = r(s(x_1 + \chi) - x_3) + U_{x3} \end{cases} \quad (7)$$

Coupled System-2:

$$\begin{cases} \frac{dy_1}{dt} = y_2 - y_1^3 + ay_1^2 - y_3 + I + U_{y1} \\ \frac{dy_2}{dt} = c - dy_1^2 - y_2 + U_{y2} \\ \frac{dy_3}{dt} = r(s(y_1 + \chi) - y_3) + U_{y3} \end{cases} \quad (8)$$

where  $U_x = [U_{x1}, U_{x2}, U_{x3}]^T$  and  $U_y = [U_{y1}, U_{y2}, U_{y3}]^T$  are the NOLCs functions. So, the errors dynamics, by taking the difference of Eqs. (7) & (8), are written as:

$$\begin{cases} \dot{e}_1 = e_2 - (\gamma y_1^3 - \delta x_1^3) + a(\gamma y_1^2 - \delta x_1^2) - e_3 + (\gamma - \delta)I + \gamma U_{y1} - \delta U_{x1} \\ \dot{e}_2 = c(\gamma - \delta) - d(\gamma y_1^2 - \delta x_1^2) - e_2 + \gamma U_{y2} - \delta U_{x2} \\ \dot{e}_3 = rs(\gamma y_1 - \delta x_1) - rs\chi(\gamma - \delta) - e_3 + \gamma U_{y3} - \delta U_{x3} \end{cases} \quad (9)$$

For stable synchronization  $e \rightarrow 0$  as  $t \rightarrow \infty$ . By substituting the conditions in Eq. (9) and taking the time derivative of Lyapunov function

$$\begin{aligned} \dot{V}(e) &= e_1 \dot{e}_1 + e_2 \dot{e}_2 + e_3 \dot{e}_3 + e_4 \dot{e}_4 = \\ &e_1 \left[ e_2 - (\gamma y_1^3 - \delta x_1^3) + a(\gamma y_1^2 - \delta x_1^2) - e_3 + (\gamma - \delta)I + \gamma U_{y1} - \delta U_{x1} \right] + \\ &+ e_2 \left[ c(\gamma - \delta) - d(\gamma y_1^2 - \delta x_1^2) - e_2 + \gamma U_{y2} - \delta U_{x2} \right] + \\ &+ e_3 \left[ rs(\gamma y_1 - \delta x_1) - rs\chi(\gamma - \delta) - e_3 + \gamma U_{y3} - \delta U_{x3} \right] \end{aligned} \quad (10)$$

we consider the following NOLC controllers:

$$\begin{cases} U_{x1} = \frac{1}{\delta} \left[ e_1 + e_2 - (\gamma y_1^3 - \delta x_1^3) \right] \\ U_{x2} = \frac{1}{\delta} c(\gamma - \delta) \\ U_{x3} = \frac{1}{\delta} rse_1 \end{cases} \quad (11)$$

and

$$\begin{cases} U_{Y1} = \frac{1}{\gamma} [e_3 - a(\gamma y_1^2 - \delta x_1^2) - (\gamma - \delta)I] \\ U_{Y2} = \frac{1}{\gamma} d(\gamma y_1^2 - \delta x_1^2) \\ U_{Y3} = \frac{1}{\gamma} rs\chi(\gamma - \delta) \end{cases} \quad (12)$$

such that

$$\dot{V}(e) = -e_1^2 - e_2^2 - e_3^2 - e_4^2 < 0 \quad (13)$$

So, Eq. (13) ensures the asymptotic global stability of synchronization.

## 2.2. Unirectional Coupling

In this section the unidirectional coupling scheme of two coupled HR systems of Eqs. (1), which is described by the following systems (14), (15), is studied.

Coupled System-1:

$$\begin{cases} \frac{dx_1}{d\tau} = x_2 - x_1^3 + a \cdot x_1^2 - x_3 + I \\ \frac{dx_2}{d\tau} = c - d \cdot x_1^2 - x_2 \\ \frac{dx_3}{d\tau} = r \cdot (s \cdot (x_1 + \chi) - x_3) \end{cases} \quad (14)$$

Coupled System-2:

$$\begin{cases} \frac{dy_1}{d\tau} = y_2 - y_1^3 + a \cdot y_1^2 - y_3 + I + U_{Y1} \\ \frac{dy_2}{d\tau} = c - d \cdot y_1^2 - y_2 + U_{Y2} \\ \frac{dy_3}{d\tau} = r \cdot (s \cdot (y_1 + \chi) - y_3) + U_{Y3} \end{cases} \quad (15)$$

where  $U_Y = [U_{Y1}, U_{Y2}, U_{Y3}]^T$  are the NOLCs functions. So, the errors dynamics, by taking the difference of Eqs. (14) & (15), are written as:

$$\begin{cases} \dot{e}_1 = e_2 - (\gamma y_1^3 - \delta x_1^3) + a(\gamma y_1^2 - \delta x_1^2) - e_3 + (\gamma - \delta)I + \gamma U_{Y1} \\ \dot{e}_2 = c(\gamma - \delta) - d(\gamma y_1^2 - \delta x_1^2) - e_2 + \gamma U_{Y2} \\ \dot{e}_3 = rs(\gamma y_1 - \delta x_1) - rs\chi(\gamma - \delta) - e_3 + \gamma U_{Y3} \end{cases} \quad (16)$$

For stable synchronization  $e \rightarrow 0$  as  $t \rightarrow \infty$ . By substituting the conditions in Eq. (16) and taking the time derivative of Lyapunov function

$$\begin{aligned}
\dot{V}(e) &= e_1\dot{e}_1 + e_2\dot{e}_2 + e_3\dot{e}_3 + e_4\dot{e}_4 = \\
&e_1 \left[ e_2 - (\gamma y_1^3 - \delta x_1^3) + a(\gamma y_1^2 - \delta x_1^2) - e_3 + (\gamma - \delta)I + \gamma U_{Y1} \right] + \\
&+ e_2 \left[ c(\gamma - \delta) - d(\gamma y_1^2 - \delta x_1^2) - e_2 + \gamma U_{Y2} \right] + \\
&+ e_3 \left[ rs(\gamma y_1 - \delta x_1) - rs\chi(\gamma - \delta) - e_3 + \gamma U_{Y3} \right]
\end{aligned} \tag{17}$$

we consider the following NOLC controllers:

$$\begin{cases}
U_{Y1} = \frac{1}{\gamma} \left[ -e_1 - e_2 + e_3 + (\gamma y_1^3 - \delta x_1^3) - a(\gamma y_1^2 - \delta x_1^2) - (\gamma - \delta)I \right] \\
U_{Y2} = \frac{1}{\gamma} \left[ -(\gamma - \delta) + d(\gamma y_1^2 - \delta x_1^2) \right] \\
U_{Y3} = \frac{1}{\gamma} \left[ -rse_1 + rs\chi(\gamma - \delta) \right]
\end{cases} \tag{18}$$

such that

$$\dot{V}(e) = -e_1^2 - e_2^2 - e_3^2 - e_4^2 < 0 \tag{19}$$

So, Eq. (19) ensures the asymptotic global stability of synchronization.

### 3. SIMULATION RESULTS

In this section the results of the simulation process in the two coupling (bidirectional and unidirectional) schemes are presented. As system's parameters, the aforementioned in section 1 ( $a = 3.1$ ,  $c = 1.2$ ,  $d = 5.8$ ,  $I = 6$ ,  $r = 0.01$ ,  $\chi = 1.9$  and  $s = 4.9$ ) have been chosen, so as each one of the coupled systems be in a chaotic mode. Also, the following initial conditions have been chosen  $(x_1, x_2, x_3)_0 = (2, 0.5, 0.08)$  and  $(y_1, y_2, y_3)_0 = (0.2, 0.1, 0.05)$ . The system's dynamic behavior is investigated numerically by employing a fourth order Runge-Kutta algorithm.

#### 3.1. Bidirectional Coupling ( $\gamma = \delta = 1$ )

Firstly, the case of bidirectional coupling is chosen while the parameters  $\gamma$ ,  $\delta$  are chosen to be equal ( $\gamma = \delta = 1$ ). This is the most studied type of coupling and also the most interesting due to its applications in

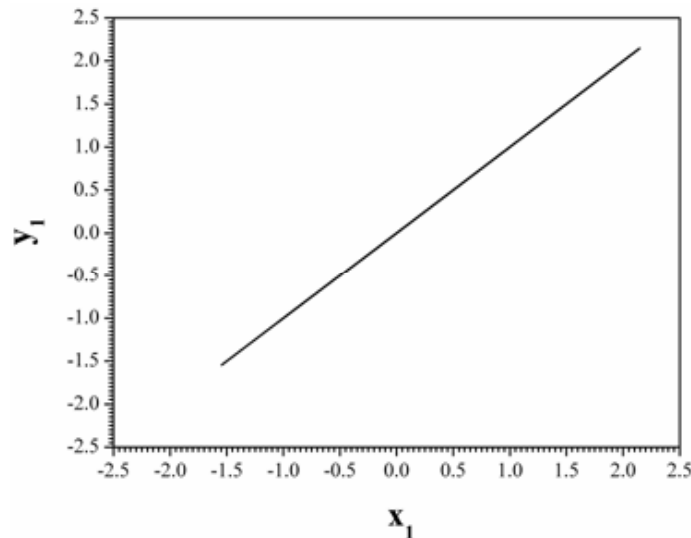


Figure 2: The phase portrait of  $y_1$  vs.  $x_1$ , for  $\gamma = \delta = 1$ , in the case of bidirectional coupling. (complete synchronization has been achieved).

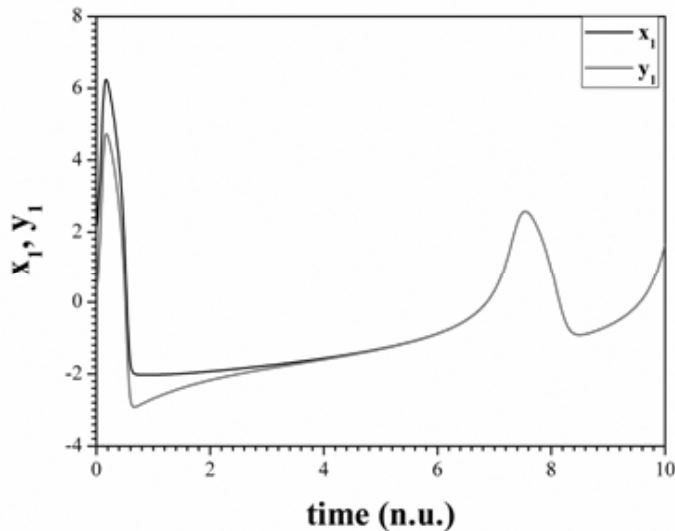


Figure 3: The time-series of  $y_1, x_1$ , for  $\gamma = \delta = 1$ , in the case of bidirectional coupling.

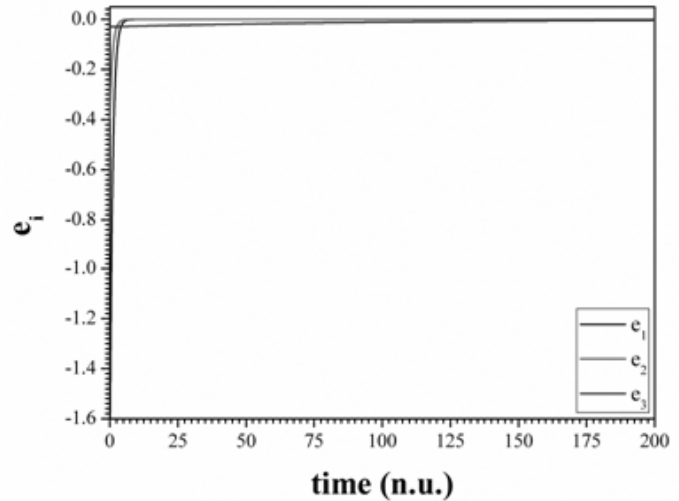


Figure 4: The plot of errors  $e_i (= \gamma y_i - \delta x_i)$ , for  $\gamma = \delta = 1$ , in the case of bidirectional coupling.

a variety of scientific fields. In this case of coupled identical chaotic systems with the proposed coupling scheme, the complete synchronization is observed. This type of synchronization is confirmed by the  $y_1$  versus  $x_1$  plot of Figure 2. Furthermore, the time-series of the variables  $x_1, y_1$  as well as the errors  $e_i$  ( $i = 1, 2, 3$ ) show the exponential convergence to zero which confirms the expected system's complete synchronization (Figures 3 & 4).

### 3.2. BIDIRECTIONAL COUPLING ( $\gamma = 1, \delta = -1$ )

By choosing the parameters of the error functions as  $\gamma = 1$  and  $\delta = -1$ , in the case of bidirectional coupling, the attractor of the first coupled system has been inverted in regard to the second one, as it is shown in Figure 5. The phase portrait of  $y_1$  versus  $x_1$  in Figure 6 indicates that the coupled system is in antisynchronization state, which is also confirmed by the time-series of  $y_1, x_1$  and the errors plot in Figures 7 & 8.

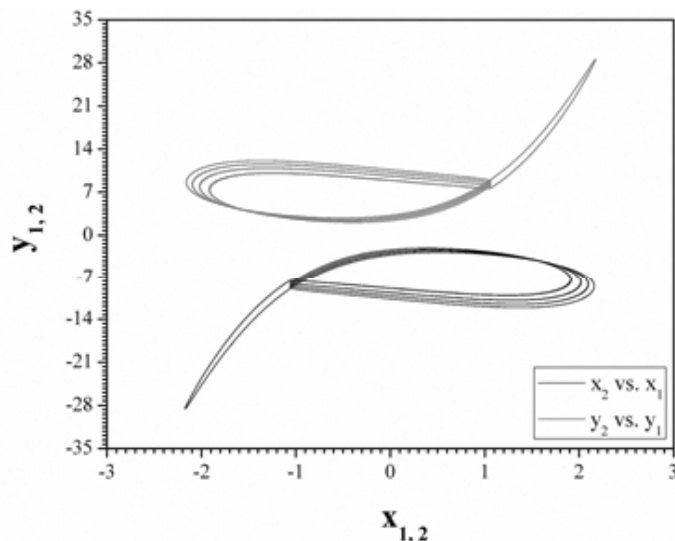


Figure 5: The phase portraits of  $x_2$  vs.  $x_1$  (black) and  $y_2$  vs.  $y_1$  (red), for  $\gamma = 1$  and  $\delta = -1$ , in the case of bidirectional coupling.

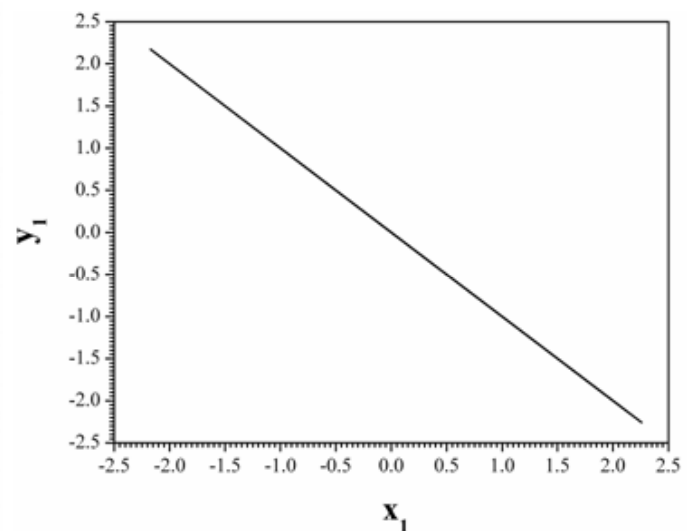


Figure 6: The phase portrait of  $y_1$  vs.  $x_1$ , for  $\gamma = 1$  and  $\delta = -1$ , in the case of bidirectional coupling. (antisynchronization has been achieved).

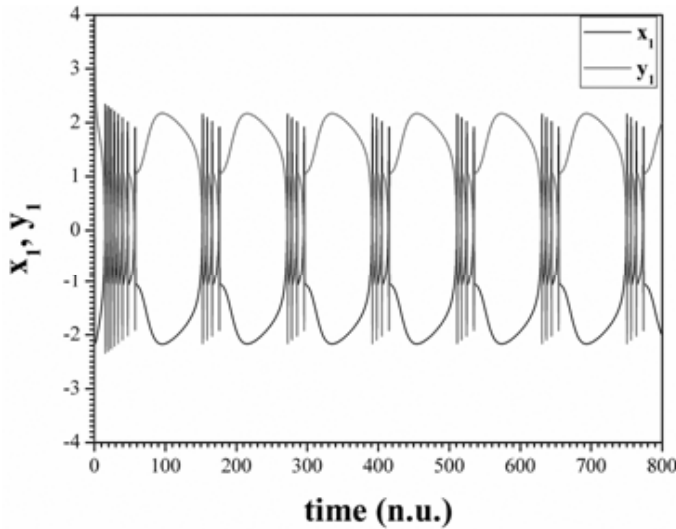


Figure 7: The time-series of  $y_1, x_1$ , for  $\gamma = 1$  and  $\delta = -1$ , in the case of bidirectional coupling.

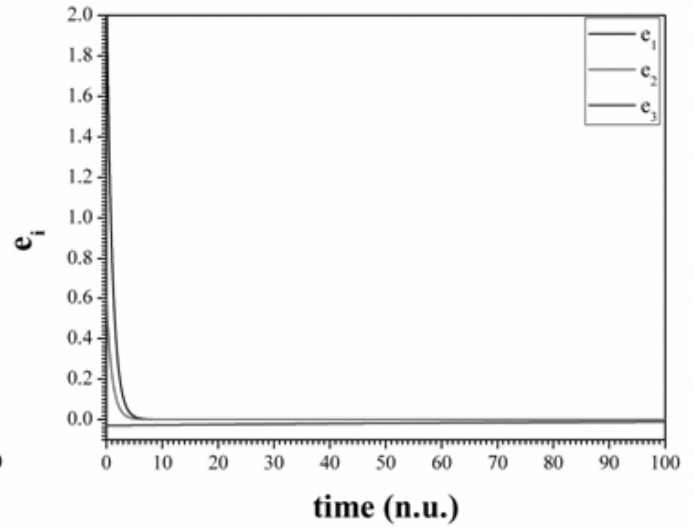


Figure 8: The plot of errors  $e_i (= \gamma y_i - \delta x_i)$ , for  $\gamma = 1$  and  $\delta = -1$ , in the case of bidirectional coupling.

### 3.3. Unirectional Coupling ( $\gamma = \delta = 1$ )

In this case, the unidirectional coupling is studied by using the same errors parameters ( $\gamma = \delta = 1$ ). With the proposed coupling scheme, the complete synchronization is observed. This type of synchronization is

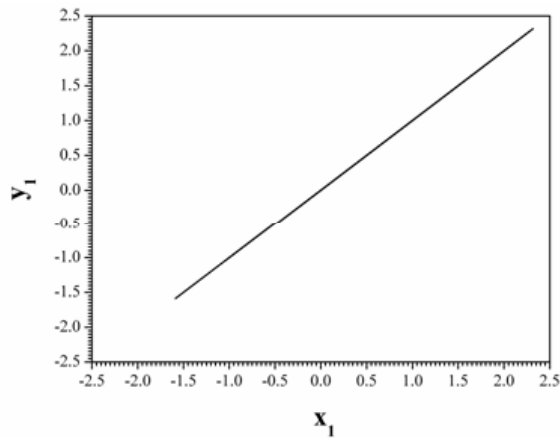


Figure 9: The phase portrait of  $y_1$  vs.  $x_1$ , for  $\gamma = \delta = 1$ , in the case of unidirectional coupling. (complete synchronization has been achieved).

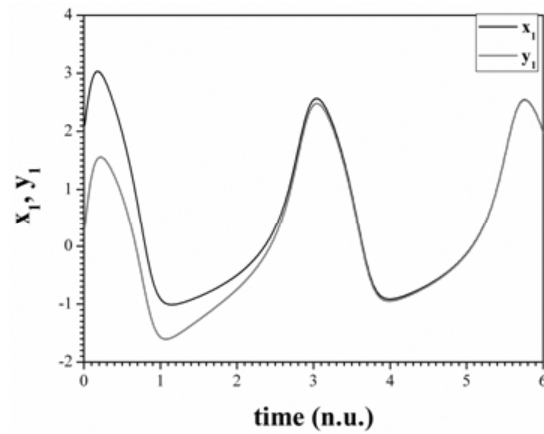


Figure 10: The time-series of  $y_1, x_1$ , for  $\gamma = \delta = 1$ , in the case of unidirectional coupling.

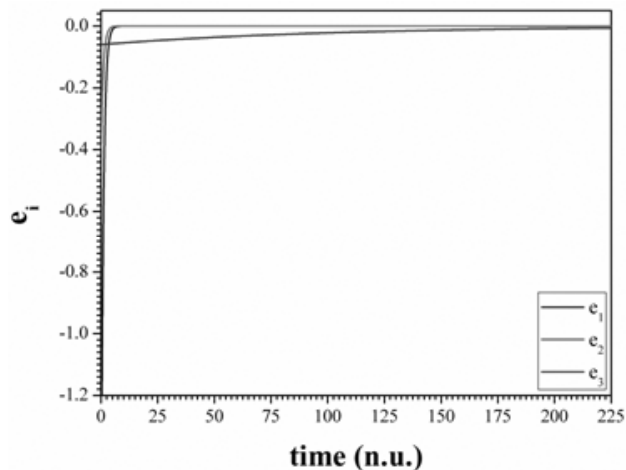


Figure 11: The plot of errors  $e_i (= \gamma y_i - \delta x_i)$ , for  $\gamma = \delta = 1$ , in the case of unidirectional coupling.

confirmed by the  $y_1$  versus  $x_1$  plot of Figure 9. Furthermore, the time-series of the variables  $x_1, y_1$  as well as the errors  $e_i$  ( $i = 1, 2, 3$ ) show the exponential convergence to zero which confirms the expected system's complete synchronization (Figures 10 & 11).

### 3.4. UNIRECTIONAL COUPLING ( $\gamma = 1, \delta = -1$ )

By choosing the parameters of the error functions as  $\gamma = 1$  and  $\delta = -1$ , in the case of unirectional coupling, the attractor of the first coupled system has been inverted in regard to the second one, as it is shown in Figure 12. The phase portrait of  $y_1$  versus  $x_1$  in Figure 13 indicates that the coupled system is in antisynchronization state, which is also confirmed by the time-series of  $y_1, x_1$  and the errors plot in Figures 14 & 15.

## 4. CIRCUIT IMPLEMENTATION

In this section, an electronic circuit is introduced to implement the HR model (1). By using a general approach with operational amplifiers [23], the designed circuit is presented in Figure 16.

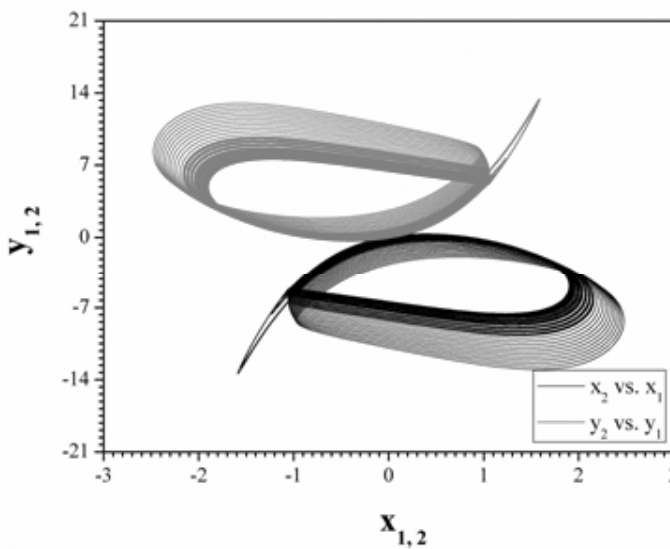


Figure 12: The phase portraits of  $x_2$  vs.  $x_1$  (black) and  $y_2$  vs.  $y_1$  (red), for  $\gamma = 1$  and  $\delta = -1$ , in the case of unirectional coupling.

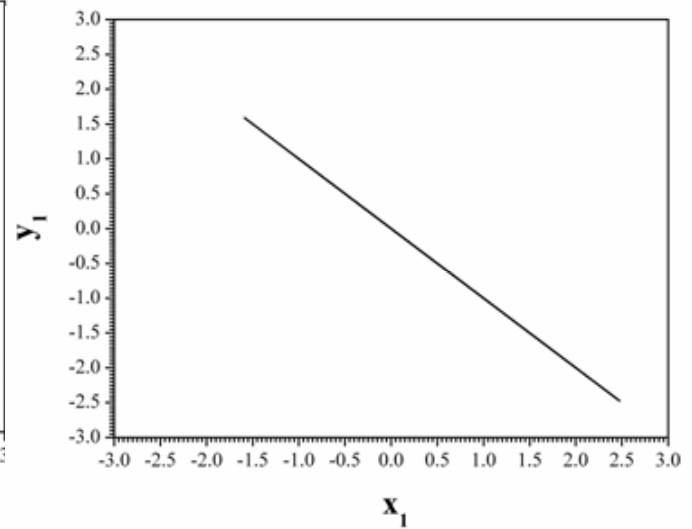


Figure 13: The phase portrait of  $y_1$  vs.  $x_1$ , for  $\gamma = 1$  and  $\delta = -1$ , in the case of bidirectional coupling. (antisynchronization has been achieved).

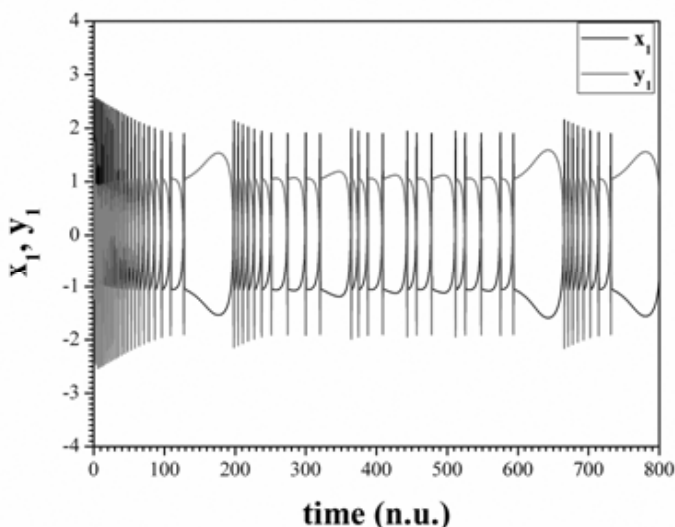


Figure 14: The time-series of  $y_1, x_1$ , for  $\gamma = 1$  and  $\delta = -1$ , in the case of bidirectional coupling.

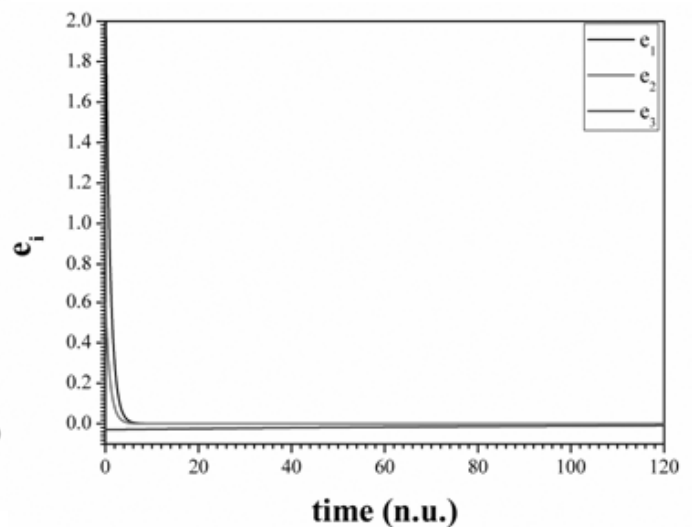


Figure 15: The plot of errors  $e_i$  ( $= \gamma y_i - \delta x_i$ ), for  $\gamma = 1$  and  $\delta = -1$ , in the case of bidirectional coupling.

By applying Kirchhoff's circuit laws, circuit equations can be written as:

$$\begin{cases} \frac{dv_{C_1}}{dt} = \frac{1}{R_1 C_1} v_{C_2} - \frac{1}{100 R_2 C_1} v_{C_1}^3 + \frac{1}{10 R_3 C_1} v_{C_1}^2 - \frac{1}{R_4 C_1} v_{C_3} - \frac{1}{R_5 C_1} V_I \\ \frac{dv_{C_2}}{dt} = -\frac{1}{R_6 C_2} V_C - \frac{1}{10 R_7 C_2} v_{C_1}^2 - \frac{1}{R_8 C_2} v_{C_2} \\ \frac{dv_{C_3}}{dt} = \frac{1}{R_9 C_3} v_{C_1} - \frac{1}{R_{10} C_3} V_x - \frac{1}{R_{11} C_3} v_{C_3} \end{cases} \quad (20)$$

where the voltages  $v_{C_1}$ ,  $v_{C_2}$ , and  $v_{C_3}$  across the capacitors  $C_1$ ,  $C_2$ , and  $C_3$  represent the variables  $X$ ,  $Y$ ,  $Z$  of HR model (1). The values of components in Figure 16 are selected as follows:  $R_1 = R_4 = R_5 = R_6 = R_8 = R = 100 \text{ k}\Omega$ ,  $R_2 = 1 \text{ k}\Omega$ ,  $R_3 = 3.226 \text{ k}\Omega$ ,  $R_7 = 1.724 \text{ k}\Omega$ ,  $R_9 = R_{10} = 2.04 \text{ M}\Omega$ ,  $R_{11} = 10 \text{ M}\Omega$ ,  $C_1 = C_2 = C_3 = 1 \text{ nF}$ ,  $V_I = -6 \text{ V}_{\text{DC}}$ ,  $V_C = -1.2 \text{ V}_{\text{DC}}$ , and  $V_x = -1.9 \text{ V}_{\text{DC}}$ , while the power supplies of all active devices are  $\pm 17 \text{ V}_{\text{DC}}$ .

The designed circuit in Figure 16 has been implemented using the electronic simulation package OrCAD. Circuitual attractors, which are depicted in Figure 17, are similar to the theoretical attractors in Figure 1.

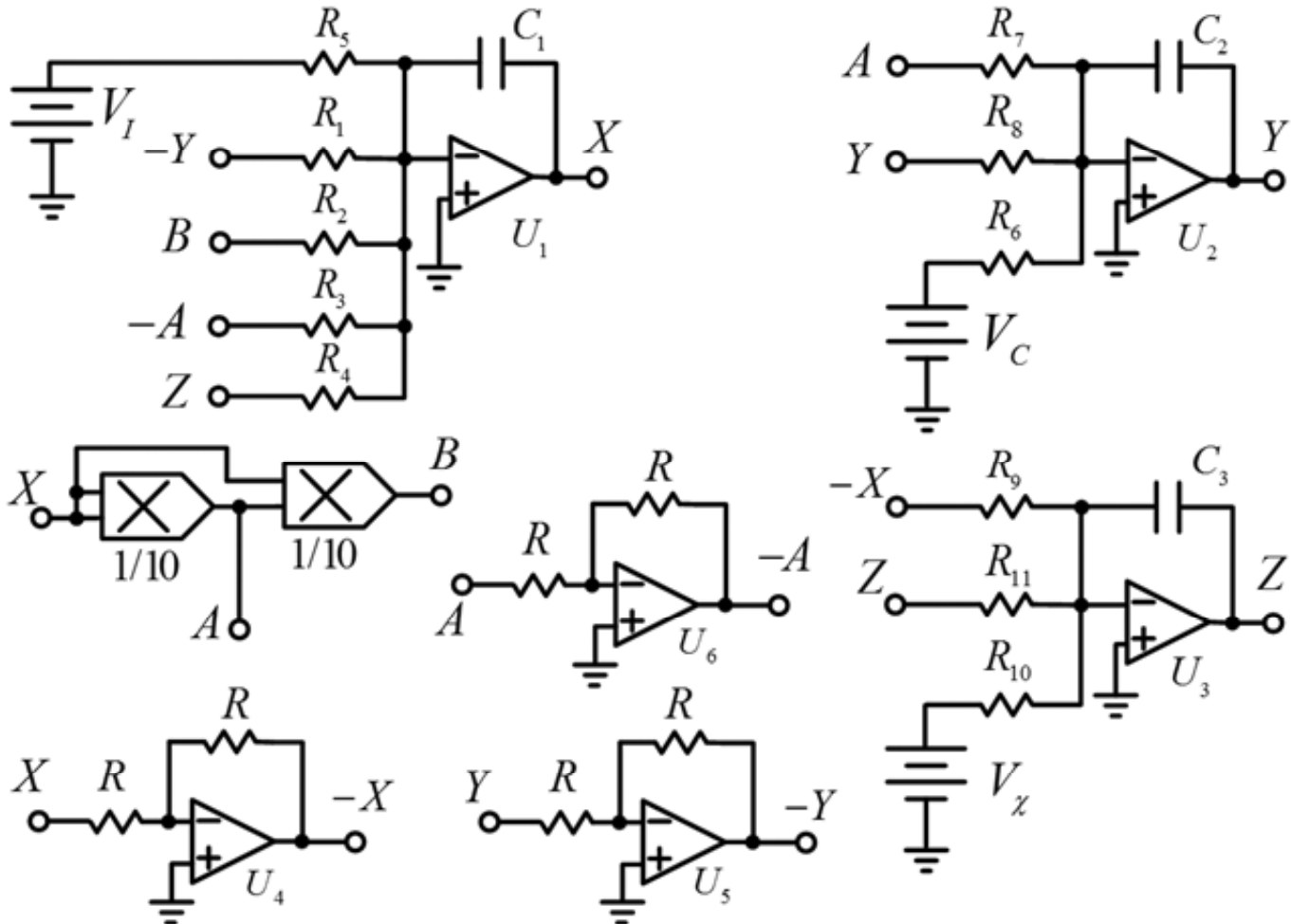
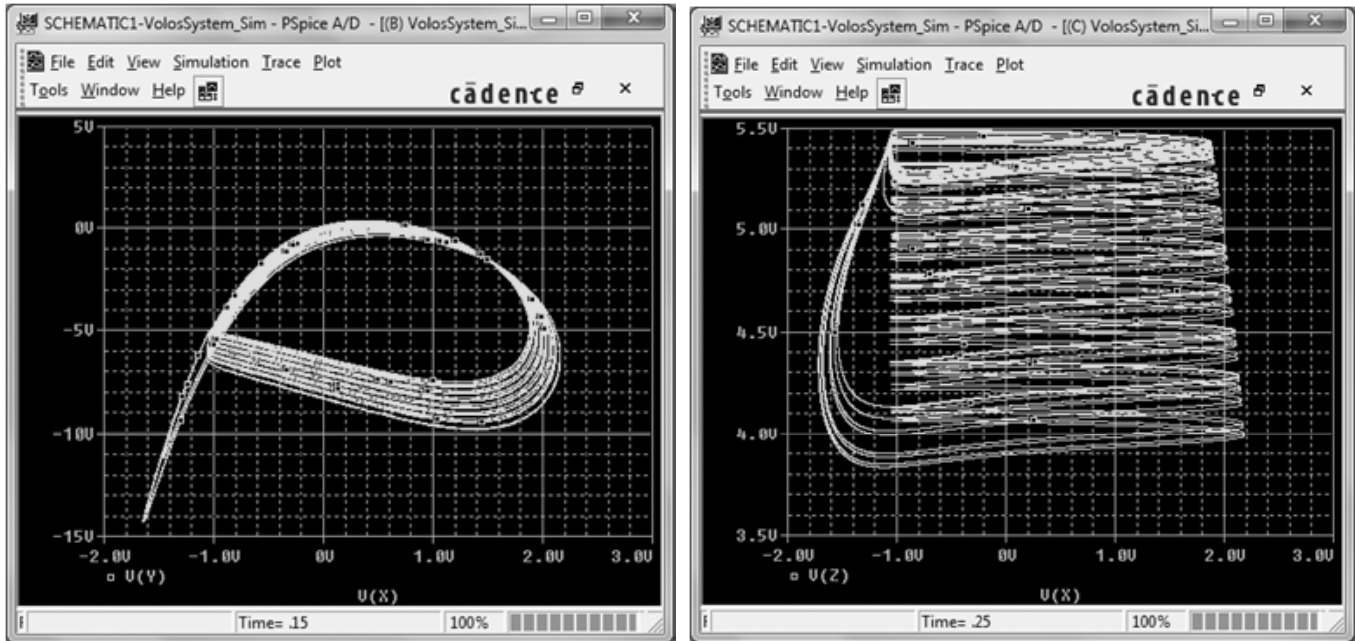
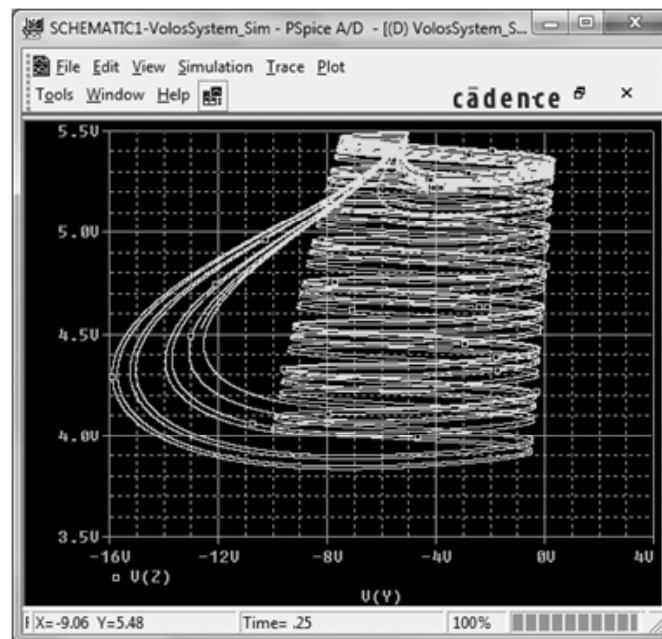


Figure 16: The schematic of the circuit which emulating HR model (1).



(a) (Continued)

(b)



(c)

Figure 17: The chaotic attractor of the designed circuit in (a)  $X - Y$  plane, (b)  $X - Z$  plane, and (c)  $Y - Z$  plane.

## 5. CONCLUSION

In this paper the case of bidirectional and unidirectional coupling scheme of two identical coupled Hindmarsh–Rose neuron models was studied. The proposed system is a three-dimensional dynamical system, which for the chosen set of parameters was in a chaotic behavior. Furthermore, the coupling method was based on a recently new proposed scheme based on the nonlinear open loop controller.

According to the simulation results from system's numerical integration, the appearance of complete synchronization and anti-synchronization, depending on the signs of the parameters of the error

functions, was investigated. So, by choosing an appropriate sign for the error functions one could drive the coupling system either in complete synchronization or anti-synchronization behavior.

As it is known, the complex behavior of chaotic neuron models, like the aforementioned, makes the control difficult in practical applications where a particular dynamic is desired. So, this paper presents an interesting research result for the Hindmarsh–Rose neuron model, because this method could be very useful in many potential applications of these systems.

Furthermore, the Hindmarsh–Rose neuron model was emulated by an electronic circuit and its dynamical behavior was studied by using the electronic simulation package Cadence OrCAD in order to confirm the feasibility of the theoretical model.

As a next step in this research direction is the application of the proposed method in non-identical coupled Hindmarsh–Rose neuron models in order to satisfy the goal of control of systems, which are in totally different dynamical behaviors.

### References

- [1] W. Gerstner and W.M. Kistler, *Spiking Neuron Models: Single Neurons, Populations, Plasticity*, Cambridge University Press, Cambridge, 2002.
- [2] E.M. Izhikevich, “Which Model to Use for Cortical Spiking Neurons?”, *IEEE Transactions on Neural Networks*, **15**(5), 1063-1070, 2004.
- [3] A.L. Hodgkin and A.F. Huxley, “A Quantitative Description of Membrane Current and its Application to Conduction and Excitation in Nerve”, *Journal of Physiology-London*, **117**, 500-544, 1952.
- [4] R. FitzHugh, “Impulses and Physiological States in Theoretical Models of Nerve Membrane”, *Biophysical Journal*, **1**, 445-466, 1961.
- [5] I.M. Kyprianidis and A.T. Makri, “Complex Dynamics of FitzHugh-Nagumo Type Neurons Coupled With Gap Junction Under External Voltage Stimulation”, *Journal of Engineering Science and Technology Review*, **6**(4), 104-114, 2013.
- [6] J.L. Hindmarsh and R.M. Rose, “A Model of Neuronal Bursting Using Three Coupled First Order Differential Equations”, In Proc. of Royal Society London, Series B, **221**, 87-102, 1984.
- [7] A.V. M. Herz, T. Gollisch, C.K. Machens and D. Jaeger, “Modeling Single-Neuron Dynamics and Computations: A Balance of Detail and Abstraction”, *Science*, **314**, 80-85, 2006.
- [8] A.S. Pikovsky, M. Rosenblum and J. Kurths, *Synchronization: A Universal Concept in Nonlinear Sciences*, Cambridge University Press, Cambridge, 2003.
- [9] E. Mosekilde, Y. Maistrenko and D. Postnov, *Chaotic Synchronization: Applications to Living Systems*, World Scientific, Singapore, 2002.
- [10] I. Szatmári and L.O. Chua, “Awakening Dynamics via Passive Coupling and Synchronization Mechanism in Oscillatory Cellular Neural/Nonlinear Networks”, *Int. J. Circ. Theor. Appl.*, **36**, 525-553, 2008.
- [11] N.H. Holstein-Rathlou, K.P. Yip, O.V. Sosnovtseva and E. Mosekilde, “Synchronization Phenomena in Nephron-Nephron Interaction”, *Chaos*, **11**, 417-426, 2001.
- [12] X. Liu and T. Chen, “Synchronization of Identical Neural Networks and Other Systems With an Adaptive Coupling Strength”, *Int. J. Circ. Theor. Appl.*, **38**, 631-648, 2010.
- [13] E. Tognoli and J.A.S. Kelso, “Brain Coordination Dynamics: True and False Faces of Phase Synchrony and Metastability”, *Prog. Neurobiol.*, **87**, 31-40, 2009.
- [14] J. Wang, Y.Q. Che, S.S. Zhou and B. Deng, “Unidirectional Synchronization of Hodgkin-Huxley Neurons Exposed to ELF Electric Field”, *Chaos Solitons Fract.*, **39**, 1335-1345, 2009.
- [15] S. Jafari, M. Haeri and M.S. Tavazoei, “Experimental Study of a Chaos-based Communication System in the Presence of Unknown Transmission Delay”, *Int. J. Circ. Theor. Appl.*, **38**, 1013-1025, 2010.
- [16] Ch.K. Volos, I.M. Kyprianidis and I.N. Stouboulos, “Experimental Demonstration of a Chaotic Cryptographic Scheme”, *WSEAS Trans. Circ. Syst.*, **5**, 1654-1661, 2006.
- [17] G. Grassi and S. Mascolo, “Synchronization of High-order Oscillators by Observer Design With Application to Hyperchaos-based Cryptography”, *Int. J. Circ. Theor. Appl.*, **27**, 543-553, 1999.

- [18] A.S. Dimitriev, A.V. Kletsovi, A.M. Laktushkin, A.I. Panas and S.O. Starkov, "Ultrawideband Wireless Communications Based on Dynamic Chaos", *J. Commun. Technol. Electron.*, **51**, 1126-1140, 2006.
- [19] H. Fujisaka and T. Yamada, "Stability Theory of Synchronized Motion in Coupled-Oscillator Systems", *Prog. Theory Phys.*, **69**, 32-47, 1983.
- [20] A.S. Pikovsky, "On the Interaction of Strange Attractors," *Z. Phys. B-Condensed Matter*, **55**, 149-154, 1984.
- [21] L.M. Pecora and T.L. Carroll, "Synchronization in Chaotic Systems", *Phys. Rev. Lett.*, **64**, 821-824, 1990.
- [22] E. Padmanaban, C. Hens and K. Dana, "Engineering Synchronization of Chaotic Oscillator Using Controller Based Coupling Design", *Chaos*, **21**, 013110, 2011.
- [23] L. Fortuna, M. Frasca and M. G. Xibilia, *Chua's Circuit Implementations: Yesterday, Today and Tomorrow*, World Scientific, Singapore, 2009.